Available online at www.sciencedirect.com
ScienceDirect
Quaternary Research 67 (2007) 487–501
QUATERNARY RESEARCH
www.elsevier.com/locate/yqres

Geomorphological, paleontological and $^{87}Sr/^{86}Sr$ isotope analyses of early Pleistocene paleoshorelines to define the uplift of Central Apennines (Italy)

Marco Mancini [a,*], Elisabetta D'Anastasio [b,c,1], Mario Barbieri [a,d], Paolo Marco De Martini [b,e,1]

[a] CNR-Istituto di Geologia Ambientale e Geoingegneria, via Bolognola 7-00138, Roma, Italy
[b] Istituto Nazionale di Geofisica e Vulcanologia, CNT, via di Vigna Murata 605, 00143, Roma, Italy
[c] Istituto Nazionale di Geofisica e Vulcanologia, Centro per la Sismologia e l'Ingegneria Sismica, via Castello d'Aquino 13, 83035, Grottaminarda (AV), Italy
[d] Università degli Studi di Roma "La Sapienza", Dipartimento di Scienze della Terra, p.le A. Moro 5-00183, Roma, Italy
[e] UMR 7516, IPG Strasbourg, EOST, Universite' Louis Pasteur, Strasbourg, France

Received 24 March 2006
Available online 28 February 2007

Abstract

The eastern border of the Middle Valley of the Tiber River is characterized by several Plio-Pleistocene paleoshorelines, which extend for about 100 km along the western margin of the Central Apennines (Italy). We studied these paleoshorelines by the means of geological and paleontological analyses and new $^{87}Sr/^{86}Sr$ isotope analyses. The youngest and uppermost paleoshorelines have been detected and mapped through detailed geologic and stratigraphic surveys, which led to the recognition of nearshore deposits, cliff breccias, alignments of *Lithophaga* borings, fossil abrasion notches and wave-cut platforms. The altitude of these paleoshorelines decreases almost regularly in the NNW–SSE direction from 480 to 220 m a.s.l. Measurements of the $^{87}Sr/^{86}Sr$ isotope ratio have been conducted on corals and mollusks collected from sediments outcropping close to the paleoshorelines. The isotopic dating results indicate numerical values that range between 0.70907 and 0.70910 all over the 100-km outcrop. These results, together with biostratigraphic data, constrain the age of the youngest paleoshorelines to 1.65–1.50 Ma. These paleoshorelines are thus considered almost isochronous, giving an estimated uplift rate of 0.34–0.17±0.03 mm/a moving from NNW to SSE. Shape, length and continuity of the 100-km-long observed movements indicate that the studied paleoshorelines are an important marker of the Quaternary uplift of the Central Apennines.

Keywords: Early Pleistocene; Shoreline; Uplift; Apennines; Italy; Sr isotope stratigraphy

Introduction

It is widely reported that since Pleistocene time the Apenninic Chain experienced a prevalent vertical tectonics, well expressed by normal faulting and by a widespread surface uplift that acted differentially along the Italian peninsula (Cinque et al., 1993; Bordoni and Valensise, 1998; Amato and Cinque, 1999; Montone et al., 1999; Galadini and Galli, 2000; D'Agostino et al., 2001; Patacca and Scandone, 2001; Valensise and Pantosti, 2001a;b; Pondrelli et al., 2002; Bartolini, 2003). Generally, the timing and amount of uplift is constrained by few geological data. Several authors, working mainly in the Southern Apennines (Cinque et al., 1993; Bordoni and Valensise, 1998; Amato and Cinque, 1999; Patacca and Scandone, 2001), suggest that this regional uplift began in early-middle Pleistocene time, although absolute or biostratigraphic datings are scarce and irregularly distributed. Moreover, the current amount of uplift is poorly determined, mainly because of the lack of precise satellite geodetic estimates. Recently, geodetic leveling data have been used to estimate current vertical movements within the Apenninic Chain, pointing out relative vertical movements with values up to 1.5–3.0 mm/a (D'Anastasio, 2004; D'Anastasio et al., 2006).

During the Quaternary, the Central Apennines experienced important extensional tectonics and volcanism after the compressional movements that had previously characterized the tectonic setting of the chain (Parotto and Praturlon, 1975;

* Corresponding author.
E-mail addresses: marco.mancini@igag.cnr.it (M. Mancini), danastasio@ingv.it (E. D'Anastasio), mbarbieri@uniroma1.it (M. Barbieri), demartini@ingv.it (P.M. De Martini).
[1] Fax: +39 06 51860507.

0033-5894/$ - see front matter © 2007 University of Washington. All rights reserved.
doi:10.1016/j.yqres.2007.01.005

Malinverno and Ryan, 1986; Patacca et al., 1992; Cavinato and De Celles, 1999). The uplift of this chain sector is poorly determined, mainly because of the scarcity of outcropping geological markers (Galadini et al., 2003; Vannoli et al., 2004). Within this framework, the inner margin of the Central Apennines has been investigated and Pleistocene paleoshorelines have been studied in detail. These features crop out along the Tyrrhenian flank of the chain, in the Middle Valley of Tiber River (Girotti and Piccardi, 1994, and references therein), and represent an important Quaternary marker that gives some indication on uplift of this chain sector. The aim of this paper is to better evaluate the amount and time of inception of the regional uplift, by means of a new estimate of the stratigraphic position, precise elevation and age determination of the paleoshorelines. The study of all these aspects is based on bibliographic review of data, original field surveys and laboratory analyses ($^{87}Sr/^{86}Sr$ isotope analyses). Calculated vertical velocities and possible implications of uplift in the study area will also be discussed.

Stratigraphic and structural setting

The study area, the Middle Valley of the Tiber River (MVT), is located about 50 km north of Rome in the Latium and Umbria regions (Fig. 1). It is a hilly, pedemontane area which widens for more than 100 km in the NNW–SSE direction, almost parallel to the axis of the Apenninic Chain. The area corresponds to the Paglia-Tevere Graben (Funiciello and Parotto, 1978), an extensional tectono-sedimentary basin developed since the late Early Pliocene. This basin is bordered to the east by the Mt. Peglia-Amerini-Narni-Sabini-Lucretili Mountains ridge (Fig. 1) (the "Peglia-Lucretili Ridge" hereafter), where Mesozoic–Cenozoic marine carbonate and siliciclastic successions crop out, and to the west by the alignment of the Quaternary Vulsini Mountains, Vico-Cimino and Sabatini Mountains Volcanic Districts.

The basin fill is composed of (1) up to 1-km-thick Pliocene–lower Pleistocene marine, transitional and continental siliciclastic deposits, which overlay the Mesozoic–Cenozoic substratum

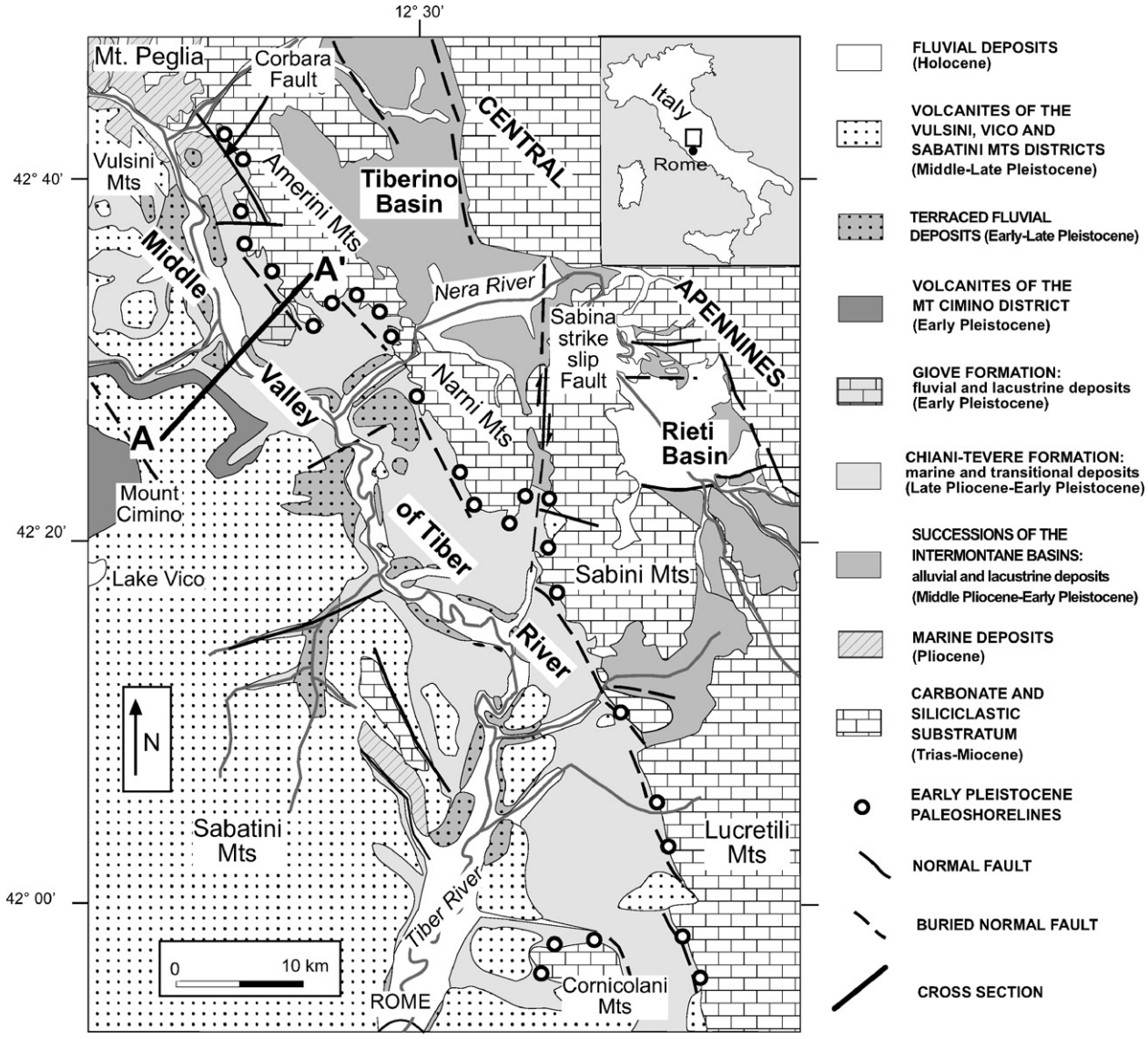

Figure 1. Geological sketch map of the Middle Valley of the Tiber river (MVT).

https://doi.org/10.1016/j.yqres.2007.01.005 Published online by Cambridge University Press

with angular unconformity; (2) younger volcanites and fluvial–lacustrine successions, which span from middle early Pleistocene to Holocene (Barberi et al., 1994; Girotti and Mancini, 2003; Mancini et al., 2004) (Fig. 2A).

The basin architecture for the Pliocene–earliest early Pleistocene is aggradational, punctuated by major progradational–retrogradational events (Mancini and Cavinato, 2005) (Fig. 2B). In this time interval, the balance between sediment basin fill and accommodation space was mainly controlled by tectonic subsidence, glacio-eustatic sea level changes and climatically driven sediment supply. The sedimentary response to all these controls is represented by two main third-order depositional sequences (Fig. 2A). The older sequence, Middle-Late Pliocene in age, is more than 500 m in thickness, is entirely composed of marine sediments, and partly corresponds to the Tenaglie-Fosso San Martino Formation (Barberi et al., 1994; Mancini et al., 2004).

The younger sequence spans from the latest Late Pliocene to the middle early Pleistocene. It is composed of (1) transgressive marine shelf, nearshore and deltaic sediments of the Chiani–Tevere Formation (CTF), up to 300 m in thickness and 2.1 to 1.5 Ma old (late Gelasian–Santernian); (2) fluvial and lacustrine deposits that fill the Tiberino and Rieti intramontane basins (Fig. 1), which are laterally contiguous to the CTF westward; (3) regressive fluvial–lacustrine carbonate and terrigenous sediments of the Giove Formation, up to 50 m in thickness and referred to the Emilian substage, i.e. middle early Pleistocene (Mancini et al., 2004). This 3rd-order sequence is composed of 4th- and 5th-order sedimentary cycles (Mancini et al., 2004) and partly corresponds to the 3.8 and 3.9 3rd-order cycles of Haq et al. (1987).

Sedimentary, paleobiologic and geomorphic markers of ancient shorelines are frequent along the eastern margin of the MVT and are referred both to the Tenaglie Fosso San Martino Formation and to the Chiani–Tevere Formation. The investigated marine paleoshorelines and their markers, both objects of this study, belong to the CTF and are located at various elevations in the basin, from about 100 to 480 m a.s.l. (Fig. 2B). They record relative sea level positions in the subsiding basin and mark progressive steps of sea level rise during the upper Gelasian–Santernian transgression. The paleoshorelines are found close to or directly on the basal bounding surface of the CTF, where it directly laps on the Mesozoic–Cenozoic substratum, or in front of prograding clastic wedges.

The uppermost palaeoshorelines (hereafter UPS, Fig. 2B) represent a group of shorelines found in the upper part of the CTF and are of particular interest for this paper. In fact, they mark the phase of maximum transgression and the highest position of relative sea level in the basin, and predate all the successive continental formations. It is likely that one of the UPS, the highest, may represent the inner edge of the maximum flooding surface (mfs) of the younger 3rd order sequence (Fig. 2B).

Moreover, the UPS postdate some early Pleistocene bioevents (Fig. 2A) that are found in the shelf sediments of the MVT (Di Bella et al., 2001; Girotti and Mancini, 2003, with references), such as the FO of the benthic and plankton forams *Bulimina etnea*, *Globigerina* aff. *G. calida calida*, *G. calabra*, *G. cariacoensis* and *Globigerinoides tenellus*. All these events occurred between 1.77 and 1.65 Ma (Pasini and Colalongo, 1994). The UPS also predate the *Hyalinaea balthica* FO event, at 1.50 Ma, which has never been discovered in the MVT basin but which is recorded in the southwestern bordering Rome Basin (Malatesta and Zarlenga, 1986). The absence of sediments bearing *H. balthica* is due to the emersion of the MVT area, occurred during the Emilian age (1.50–1.19 Ma), and to the consequent southwestward drift of marine and coastal facies (Girotti and Mancini, 2003; Mancini and Cavinato, 2005).

For the late early Pleistocene–Holocene time interval the basin architecture is composed of a series of cyclic aggradational–degradational valley fills, resulting from the concomitant effect of regional uplift, climate-driven fluvial and lacustrine sedimentation and volcanic activity (Mancini and Cavinato, 2005). The oldest deposit of this syn-uplift phase is the *Peperino* Formation, a 1.30-Ma-old rhyodacitic ignimbrite, belonging to the Mt. Cimino Volcanic District (Fig. 2A), which forms a well-preserved tabular plateau, presently at 250–270 m a.s.l. It follows (1) a staircase of four aggradational fluvial terraces of the Tiber River, flanking the Holocene alluvial plain and representing a relevant feature of uplift; and (2) a wide volcanic cover, belonging to the Vulsini Mountains, Vico and Sabatini Mountains Volcanic Districts and dated between 0.6 and 0.1 Ma (Barberi et al., 1994) (Figs. 1 and 2).

Each aggradational fluvial terrace is composed of channel-related and floodplain facies and is covered and chronologically constrained by progressively younger volcanic products (Fig. 2A). The first fluvial terrace spans from 1.2 to 0.6 Ma, the second from 0.5 to 0.3 Ma, the third is about 200–150 ka old and the fourth is late Pleistocene in age (see also Mancini and Cavinato, 2005, for further details). Moreover, the tread of each terrace gently and regularly decreases in elevation along the NNW–SSE direction. In particular, the first terrace dips from 330 to 170 m a.s.l.; the second from 210 to 65 m; the third from 100 to 35 m; the fourth from 70 to 25 m.

The main structural elements in the area are faults, strictly related to the extension and uplift of the MVT basin and to volcanism (Locardi et al., 1977; Funiciello and Parotto, 1978; Barberi et al., 1994; Cavinato et al., 1994). Four systems of faults are recognized (Mancini and Cavinato, 2005): (1) a system of NNW–SSE trending, west-dipping high angle normal faults, which borders the "Peglia-Lucretili Ridge" to the west (the Corbara Fault (Fig. 1), mentioned in the following, pertains to this system and dissects the CTF); (2) an antithetic system of normal faults covered by the middle Pleistocene volcanites; (3) a SW–NE trending system of faults, which dissect the first terrace; and (4) the Sabina Fault, a N10°E-trending fault located in the eastern part of the basin (Fig. 1), which evolved in Neogene time from right-lateral strike slip fault to normal fault (Alfonsi et al., 1991). Within the MVT basin, most of the tectonic displacement is due to the activity of the NNW–SSE trending faults, and occurred in Pliocene and early Pleistocene times. In particular, for the early Pleistocene time interval, vertical displacement of the west-dipping normal faults do not exceed 150 m as a whole (Mancini, 2000; Mancini and Cavinato, 2005).

https://doi.org/10.1016/j.yqres.2007.01.005 Published online by Cambridge University Press

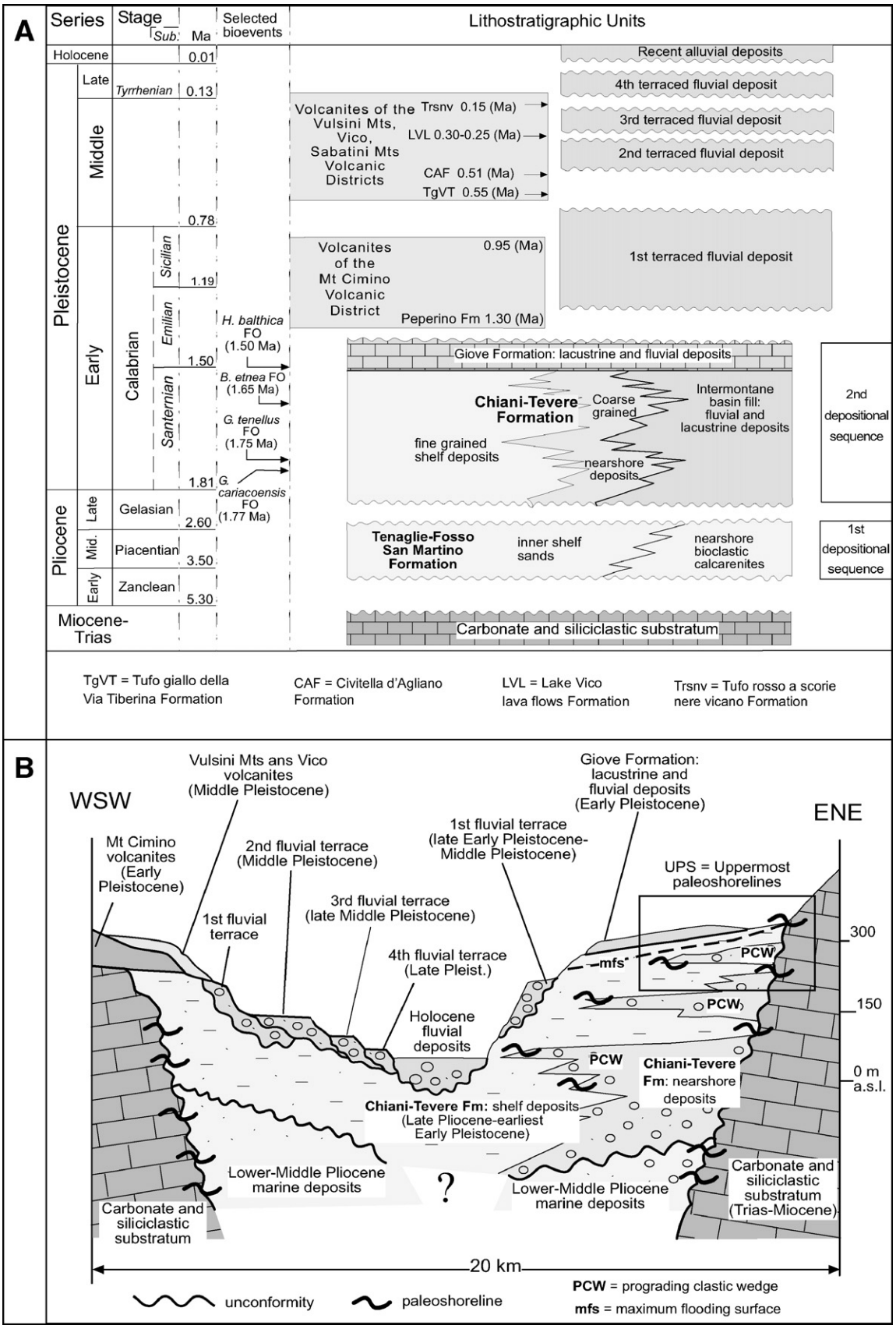

Figure 2. (A) Litho-chronostratigraphic scheme of the MVT (partly modified after Mancini and Cavinato, 2005); (B) A–A′ cross-section (not to scale) (see Fig. 1); note the stratigraphic and altimetric position of the uppermost early Pleistocene paleoshorelines (UPS).

https://doi.org/10.1016/j.yqres.2007.01.005 Published online by Cambridge University Press

Methodology and data set

Several sea level markers of geomorphic, sedimentary and paleobiologic nature have been detected within the Chiani–Tevere Formation (Figs. 3A–D). The occurrence and richness of different kinds of markers derive from the variety and lateral continuity of paleoenvironments. These are located along, in front of or inshore of the ancient coastline and developed in a marine microtidal regime. Recognized paleoenvironments are rocky coasts, shallow water fluvial and wave-dominated coarse-grained deltaic systems, lagoon-barrier island systems, beach ridge strandplains, small fan deltas and pocket beaches (Ambrosetti et al., 1987; Girotti and Piccardi, 1994; Girotti and Mancini, 2003).

In order to deal with the UPS and the laterally associated nearshore deposits, a selection of literature data has been accomplished (Ambrosetti et al., 1987; Cosentino et al., 1993; Girotti and Piccardi, 1994; Mancini et al., 2004), followed by consequent campaigns of geologic and geomorphologic survey, in order to find new outcrops and possible tectonic displacements. The whole data set is composed of 71 previously known and new sites (Table 1 and Fig. 4), each labeled with the type of detected marker and the topographic and geographic position. A description of markers is provided in the next three sections.

Geomorphic markers

The stratigraphic boundary between the CTF and the carbonate bedrock is marked by an abrupt lateral variation of the topographic gradient. The bedrock topographic surface dips from vertical to a mean dip of 15–20°, while the top surface of the CTF dips less than 5° in the SW direction. In some cases the steep bedrock surface passes seaward to the west to sub-horizontal or gently dipping surfaces, carved into the carbonate. These surfaces are few tens of meters wide and are interpreted as wave-cut terraces (Fig. 3A) bordering paleocliffs. They formed after cliff retreat, from the combined effects of mechanical wave action above the mean wave base level (wave shock, hammering, compression of air between water and shore, hydrostatic pressure), chemical weathering by mixing of fresh and sea waters, subaerial weathering and bioerosion (Summerfield, 1991; Reading and Collinson, 1996; Burbank and Anderson, 2001). In general, wave-cut terraces are formed when the rates of rock uplift equal those of eustatic sea level rise and are best preserved in areas of slow uplift (Lajoie, 1986).

In the MVT area, at the inland termination of terraces, well-preserved tidal notches are also found, which are 2 m in height and bored by lithodomous organisms (Fig. 3B). They precisely mark the ancient sea level within the intertidal zone, with a

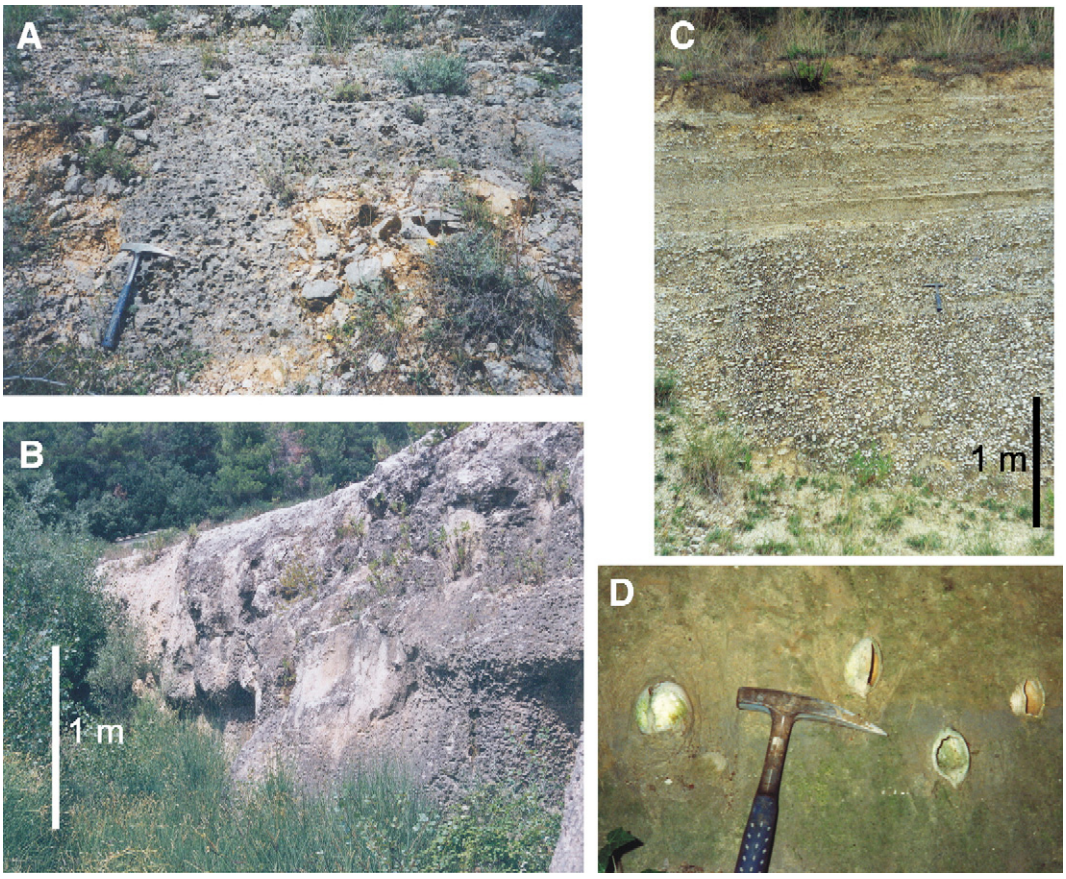

Figure 3. Geomorphic, sedimentary and paleobiologic markers of the early Pleistocene paleoshorelines: (A) wave-cut platform bored by lithodomous borings, from site 93 of Table 1; (B) tidal notch, from site 85; (C) clinostratified gravel of the beachface environment; (D) sampled molluscs for isotopic analyses from transition offshore–shoreface silt of the Chiani–Tevere Formation: *S. brocchii* in living position.

https://doi.org/10.1016/j.yqres.2007.01.005 Published online by Cambridge University Press

Table 1
Geographic and topographic positions of the selected paleoshorelines

Identification number	Site	Longitude (E, ED 1950)	Latitude (N, ED 1950)	Elevation m a.s.l.	Marker[a]	Reference[b]
3	Montecchio	12° 17′ 02″	42° 39′ 51″	375	pc, i	1
4	Montecchio	12° 17′ 15″	42° 39′ 48″	375	pc, i	1
5	La Conserva	12° 17′ 29″	42° 39′ 42″	370	gbs, f	1
8	Tenaglie	12° 17′ 02″	42° 39′ 59″	375	pc, i	2
9	Tenaglie	12° 17′ 14″	42° 39′ 14″	380	wcp, i	2
11	Fratta	12° 17′ 43″	42° 39′ 03″	400	pc, i	2
12	Il Monastero	12° 17′ 58″	42° 39′ 10″	380	pc, cb, f, i	2
13	Il Monastero	12° 17′ 55″	42° 39′ 12″	380	pc, cb, f, i	2
14	Madonna delle Grazie	12° 17′ 11″	42° 38′ 36″	375	pc, cb, f, i	2
19	Porchiano	12° 21′ 08″	42° 32′ 28″	375	pc, i	2
20	Poggio Genzano	12° 21′ 28″	42° 32′ 39″	370	pc, cb, i	2
21	Porchiano	12° 22′ 50″	42° 32′ 20″	360	pc, cb, i	2
22	Monte Pelato	12° 23′ 11″	42° 32′ 21″	350	pc, i	2
24	Podere Monte Piglio	12° 25′ 14″	42° 34′ 53″	350	pc, cb, i	2
25	Podere Picchi	12° 25′ 45″	42° 34′ 43″	360	pc, i	2
26	Podere Pervito	12° 25′ 39″	42° 34′ 29″	350	pc, i	2
27	Podere Beato	12° 24′ 04″	42° 34′ 01″	375	pc, i	2
29	La Gioiosa	12° 23′ 47″	42° 33′ 13″	350	pc, cb, i	2
32	Il Macello	12° 24′ 48″	42° 33′ 13″	360	pc, i	2
41	Montenero	12° 24′ 04″	42° 32′ 00″	340	pc, cb, i	2
42	Fornole	12° 27′ 23″	42° 32′ 42″	350	gbs, f	2
66	Poggio	12° 32′ 59″	42° 25′ 09″	325	wcp, i	2
67	Aravecchia	12° 33′ 17″	42° 25′ 12″	375	pc, cb, i	2
68	Aravecchia	12° 33′ 18″	42° 25′ 13″	375	pc, cb, i	2
69	Aravecchia	12° 33′ 21″	42° 25′ 12″	375	pc, cb, i	2
72	Madonna della Neve	12° 35′ 50″	42° 22′ 16″	350	cb, i	2
74	Case Bernacchia	12° 35′ 37″	42° 22′ 26″	355	pc, cb, i	2
76	Case Piano Selve	12° 35′ 09″	42° 22′ 56″	365	pc, i	2
77	Casale Agrippina	12° 35′ 13″	42° 22′ 48″	350	cb, i	2
78	Santa Maria Maddalena	12° 34′ 53″	42° 23′ 19″	350	pc, cb, i	2
79	Santa Maria Maddalena	12° 34′ 37″	42° 23′ 24″	350	pc, cb, i	2
80	Santa Maria Maddalena	12° 34′ 29″	42° 23′ 35″	350	pc, cb, i	2
81	Santa Maria Maddalena	12° 34′ 22″	42° 23′ 45″	375	pc, i	2
82	Santa Maria Maddalena	12° 34′ 20″	42° 23′ 50″	375	pc, i	2
85	Calvi dell′Umbria	12° 34′ 20″	42° 24′ 07″	350	n, gbs, f, i	2
86	Calvi dell′Umbria	12° 34′ 11″	42° 24′ 06″	340	cb, i	2
89	Sant′Andrea	12° 34′ 03″	42° 24′ 27″	375	n, wcp, gbs, f, i	2
90	Calvi dell′Umbria	12° 34′ 01″	42° 24′ 29″	380	pc, cb, i	2
93	Montagnola	12° 37′ 54″	42° 21′ 51″	350	wcp, gbs, i	2
94	Montagnola	12° 37′ 54″	42° 21′ 54″	350	wcp, gbs, i	2
95	San Sebastiano	12° 38′ 26″	42° 21′ 49″	370	pc, cb, i	2
96	Vacone	12° 39′ 06″	42° 23′ 06″	390	pc, i	2
97	Vacone	12° 39′ 15″	42° 23′ 12″	375	pc, cb, i	2
98	Cima Boschetto	12° 39′ 21″	42° 23′ 19″	375	pc, cb, i	2
99	Colle Castagna	12° 41′ 21″	42° 22′ 23″	390	cb, i	2
100	Colle Castagna	12° 41′ 05″	42° 23′ 41″	480	cb, i	2
101	Fonte Castelletto	12° 41′ 45″	42° 23′ 41″	440	cb, i	2
102	Scoppieto	12° 17′ 54″	42° 43′ 36″	445	gbs, f	1
103	Civitella del Lago	12° 17′ 20″	42° 43′ 06″	460	pc, cb, i	1
104	Santa Caterina	12° 16′ 47″	42° 41′ 43″	380	gbs, f	1
106	Cioppi	12° 41′ 20″	42° 23′ 22″	470	lp, f	3
107	Casperia	12° 41′ 10″	42° 20′ 37″	320	cb, i	3
108	Cesola	12° 41′ 00″	42° 19′ 37″	315	pc, i	3
109	Monte Fiolo	12° 40′ 09″	42° 19′ 48″	310	cb, i	3
110	Poggio Catino	12° 41′ 27″	42° 17′ 32″	285	lp, f	3
111	Pomonte	12° 42′ 22″	42° 13′ 12″	275	wcp	3
112	Prime Case	12° 43′ 20″	42° 12′ 45″	290	pc, i	3
113	Fara in Sabina	12° 43′ 27″	42° 12′ 34″	270	pc, cb, i	4
116	Moricone	12° 46′ 11″	42° 07′ 06″	250	pc, i	3
117	Convento Passionisti	12° 46′ 17″	42° 07′ 01″	245	pc, i	3
118	Colle Palombaro	12° 46′ 11″	42° 06′ 53″	230	pc, i	3
119	Cavalieri	12° 46′ 18″	42° 06′ 30″	225	cb, i	3
120	Palombara Sabina	12° 46′ 34″	42° 05′ 16″	255	cb, i	3
121	Fosso Casale Rosso	12° 47′ 20″	42° 01′ 45″	220	pc, cb, i	3

https://doi.org/10.1016/j.yqres.2007.01.005 Published online by Cambridge University Press

Table 1 (*continued*)

Identification number	Site	Longitude (E, ED 1950)	Latitude (N, ED 1950)	Elevation m a.s.l.	Marker [a]	Reference [b]
123	Fosso Vannoni	12° 47′ 56″	42° 01′ 19″	230	pc, i	3
125	Fonte Paoloni	12° 48′ 04″	42° 01′ 14″	230	pc, i	3
126	Fosso Vena	12° 47′ 49″	42° 01′ 04″	235	pc, cb, i	3
128	Fonte	12° 43′ 24″	42° 02′ 06″	220	pc, i	3
130	Poggio Cesi	12° 43′ 42″	42° 01′ 50″	250	pc, i	3
131	Poggio Cesi	12° 43′ 53″	42° 01′ 45″	250	pc, i	3
132	Fonte Santa Lucia	12° 43′ 53″	42° 01′ 45″	250	cb, i	3

[a] Selected markers: pc=paleocliff; wcp=wave cut platform; n=abrasion notch; cb=cliff breccia; gbs=gravely–sandy beach deposit; lp=lagoon pelite; i=ichnofossils; f=body fossils.
[b] References: 1=Ambrosetti et al. (1987); 2=Girotti and Piccardi (1994); 3=original data; 4=Cosentino et al. (1993).

±0.5 m error (Nisi et al., 2003), and record episodes of relative sea level stillstand (Antonioli et al., 2006). Commonly both wave-cut platforms and notches are preserved by few-meter-thick cover of cliff breccias or sandy pocket beach deposits (see below).

Several small fan deltas, less than 0.5 km^2 wide, are present along the western margin of the "Peglia-Lucretili Ridge", in correspondence of narrow NE–SW-oriented valleys (Girotti and Piccardi, 1994; Girotti and Mancini, 2003). They form wedges dipping 6–10° to the west, from the apex, at about 450–500 m, to the toe at 300–350 m a.s.l. Fan deltas laterally pass seaward to the sub-horizontal sandy deposits of the CTF; related sediments are described in the next section.

Sedimentary markers

Cliff breccia deposits

Crudely stratified subrounded and poorly sorted large boulders and cobbles are present at the toe of the paleocliffs and above some of the wave-cut platforms. They are in general enclosed in sandy–clayey matrix. These deposits are interpreted as cliff breccias, derived from rock falls and avalanches after abrasion and quarrying of the substratum. Rapid burial prevented the mature sorting of sediments and the removal of fines by wave action. Boulders are in some cases bored by entofauna, with borings on a single side. The breccia interfingers seaward with shoreface sand.

Pocket beach deposits

These deposits are formed by well-sorted fine sands, with planar, horizontal or gently dipping seaward laminations. They contain rare fossils, mostly barnacles and *Ostrea*, and burrows of the *Skolithos* ichnogenus. Lamina sets are commonly truncated by reactivation surfaces, caused by wave action on the beach. They formed in the intertidal zone and are found on small embayments or above wave-cut platforms.

Fan-delta deposits

Fan-delta deposits are clast supported and are composed of poorly sorted gravels, subangular in shape and organized into alternating massive tabular bodies and channel lenses, a few meters thick. The gravels are rich in clayey–sandy matrix, in some cases with an open framework. Gravels interfinger downslope with shoreface sands. The position of the ancient shorelines is inferred at various levels of the fans by alignments of clasts bored by lithodomous organisms and by the presence of ostreids (Girotti and Piccardi, 1994).

Gravely sandy shoreface and beachface deposits

These deposits are formed by coarsening up successions of lithofacies, from 2 to 10 m thick, which are bounded at the base and top by flooding surfaces. From bottom to top, outcrops show (1) bioturbated massive, silty sands of the shoreface–offshore transition and of the lower shoreface environments; (2) upper shoreface cross-bedded coarse sand, interfingered landward with wedges and lenses of massive gravel; (3) clinostratified, seaward-dipping cobbles and pebbles, well rounded and sorted, of the lower beachface sub-environment (Massari and Parea, 1988); and (4) horizontally stratified fine

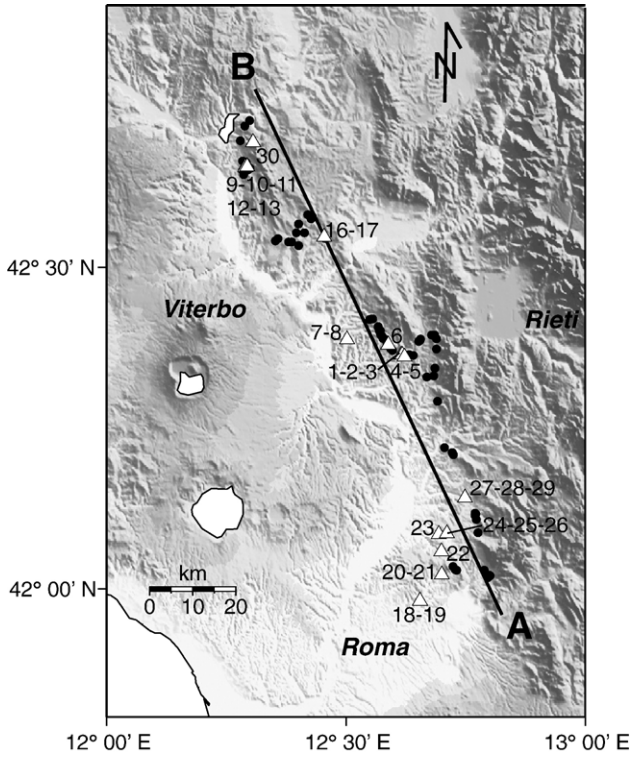

Figure 4. Location of the uppermost paleoshoreline (UPS) markers (black dots) and sites of sampling for Sr isotope analyses (white triangles). Site numbers are referred to Table 2. A–B trace is referred to Figure 6.

https://doi.org/10.1016/j.yqres.2007.01.005 Published online by Cambridge University Press

cobbles and pebbles commonly seaward imbricated of the upper beachface (Fig. 3C). The latter forms close to mean sea level (Bardaj et al., 1990). All the successions represent progradational gravely–sandy beachface successions, which formed in front of shallow water, wave-dominated, fluvio-deltaic and coastal plain systems (Mancini, 2000; Mancini and Cavinato, 2005).

Lagoon deposits

These deposits are composed of massive or thinly laminated pelites, sometimes interbedded with peat or fine sandy horizons, from few to few tens of meters thick, embedded into sandy and gravely fluvio-deltaic and nearshore deposits.

Paleobiologic markers

Paleobiologic markers, both body and trace fossils, are very frequent in the CTF along the paleoshorelines and in the associated shallow marine and lagoonal sediments.

In the gravely–sandy beachface and shoreface deposits, and more rarely in the cliff breccia, the only fossils that are present include *Balanus* spp., *Ostrea edulis* and *Anomia ephippium*. Barnacles in general indicate the mid-littoral and upper sublittoral zone (Nybakken, 2001), while molluscs are only found in the sublittoral zone and are associated with rare armored burrows ichnofossils. No body fossils are found on paleocliffs.

Very frequent molluscs and corals are found in the lower shoreface and in the transition shoreface/offshore silty sands and are commonly preserved in life position (Fig. 3d). This association is composed of bivalves (*Sinodia brocchii*, *Panopea glycimeris*, *Ostrea lamellosa*, pectinids), gastropods (*Natica tigrina*, *Bela harpula*) and the coral *Cladocora coespitosa*. These organisms characterize the infralittoral zone; corresponding paleobathymetries are in the range of 0 and −25 m a.s.l., in the Pliocene–Pleistocene basins of central Italy (Malatesta, 1974).

In the lagoon deposits, an oligotypic *in situ* taphocoenosis is found and is represented by *Cerastoderma glaucum*, *Bittium deshayesi*, *Hydrobiidae* and *Melanopsis affinis*, all organisms living in the basin-lagoon environment few meters below sea level and able to tolerate low-salinity water (Malatesta, 1974; Ciangherotti et al., 1998; Little, 2000; Nisi et al., 2003).

Of great importance in recognizing ancient shorelines are the trace fossils bored by endolithic organism, both on cliffs and clasts. In particular there are recognized the ichnofossils: *Gastrocaenolithes torpedo*, *Gastrocaenolithes* isp., *Entobia* isp., *Caulostrepsis taeniola* and *Trypanites* isp. The deep-tier boring *G. torpedo* is very common on cliffs, abrasion platform and notches (Figs. 3A, B) and was presumably produced by the bivalve *Lithophaga lithophaga* in a belt between 0 and −10 m below sea level (De Gibert et al., 1998). The *C. taeniola* and *Entobia* were bored by polychaete worms and by sponges, respectively, and are common on cliff breccia (see also Girotti and Piccardi, 1994). All the assemblage is referred to as the *Entobia* ichnofacies (Bromley and Asgaard, 1993), which characterizes cliffs and related coarse-grained deposits at the toe, just below sea level (De Gibert et al., 1998).

Sr isotope chronostratigraphy

Marine molluscs and corals were collected for $^{87}Sr/^{86}Sr$ isotope analysis from various sites in the MVT basin (Table 2) (Fig. 4). In general, sites of sampling are located along the paleoshorelines or close to them, where shallow marine sediments crop out. In a few cases, sampling sites are up to 4 km from the ancient coastline or tens of meters below the UPS. Sampled fossils are not reworked, belong to nearshore environments, are from beachface to the shoreface–offshore transition and indicate depths of up to 25 m below sea level. No fossils from brackish-water environments were collected in order to avoid measurements not referable to clearly marine environment.

Sr isotope ratios were measured on 15 mg of calcitic or aragonitic shell fragment for each specimen. Each fragment was washed ultrasonically in ultrapure water, gently crushed and rewashed in distilled water to separate the organic and pelitic residues from carbonate. Each sample was dissolved in 2.5 N ultrapure HCl, centrifuged and loaded onto a cation-exchange resin. Sr was collected as Sr $(NO_3)_2$ and put on a tungsten double-filament of a multicollector mass spectrometer.

The $^{87}Sr/^{86}Sr$ ratio has been normalized to $^{88}Sr/^{86}Sr = 0.1194$ and SRM-987 = 0.71024, based on the value of SRM-987 determined for the particular series of runs on the mass spectrometer (Hodell et al., 1990). For each specimen, 200 ratios were collected with errors expressed as two standard errors of the mean ($\pm 2 \times 10^{-5}$).

Table 2 plots the sampled specimens, the geographic and altimetric position of the site of sampling and the resultant $^{87}Sr/^{86}Sr$ ratio. Measured numerical values of the $^{87}Sr/^{86}Sr$ ratio range between 0.70907 ± 0.00002 and 0.70910 ± 0.00002 (Fig. 5). The age of the analyzed material is between 1.90 and 1.34 Ma. This is based on the regression equation of Hodell et al. (1990), where:

$$\text{age} = -0.132 \times \delta\ ^{87}\text{Sr}$$

$$\text{with } \delta\ ^{87}\text{Sr} = \left(\frac{(^{87}\text{Sr}/^{86}\text{Sr})_{\text{sample}}}{(^{87}\text{Sr}/^{86}\text{Sr})_{\text{seawater}}} - 1 \right) \cdot 10^5$$

$$\text{and } \ ^{87}\text{Sr}/^{86}\text{Sr}_{\text{seawater}} = 0.709172.$$

Discussion

Age and position of the selected paleoshorelines and uplift rate calculation

The results of the $^{87}Sr/^{86}Sr$ isotopic measurements on nearshore fossils indicate that the UPS markers represent a fairly short time interval (560 ka) over the 100-km-long outcrop. The isotopic age of the fossils, and thus of the containing sediments and of the nearby shoreline, is 1.90–1.34 Ma. Moreover, the age of UPS, based on benthic forams biostratigraphy, is between 1.65 Ma (*B. etnea* FO) and 1.50 Ma (*H.*

https://doi.org/10.1016/j.yqres.2007.01.005 Published online by Cambridge University Press

Table 2
Measured values of the $^{87}Sr/^{86}Sr$ ratio on sampled molluscs and corals from marine deposits

Sample	Analyzed species	Site	Longitude (E, ED 1950)	Latitude (N, ED 1950)	Elevation (m a.sl.)	$^{87}Sr/^{86}Sr$
GIR 1	*O. edulis*	Montagnola	12° 36′ 54″	42° 21′ 51″	350	0.70910
GIR 2	*O. edulis*	Montagnola	12° 36′ 54″	42° 21′ 51″	350	0.70907
GIR 3	*S. brocchii*	Villa Camuncini	12° 37′ 05″	42° 21′ 51″	345	0.70908
GIR 4	*P. glycimeris*	Colle Bernocchi	12° 37′ 21″	42° 21′ 40″	345	0.70909
GIR 5	*O. lamellosa*	Colle Bernocchi	12° 37′ 21″	42° 21′ 40″	345	–
GIR 6	*O. edulis*	San Donato	12° 35′ 19″	42° 22′ 49″	320	0.70908
GIR 7	*N. tigrina*	Colle Elmo	12° 30′ 07″	42° 23′ 17″	250	0.70910
GIR 8	*Chlamys varia*	Colle Elmo	12° 30′ 07″	42° 23′ 17″	250	0.70908
GIR 9	*O. edulis*	Fosso Carnano	12° 17′ 24″	42° 39′ 16″	360	–
GIR 10	*C. coespitosa*	Fosso Carnano	12° 17′ 24″	42° 39′ 16″	360	0.70908
GIR 11	*C. coespitosa*	Fosso Carnano	12° 17′ 24″	42° 39′ 16″	360	0.70909
GIR 12	*O. edulis*	Colle Pranzuto	12° 17′ 37″	42° 39′ 21″	380	0.70907
GIR 13	*O. edulis*	Colle Pranzuto	12° 17′ 37″	42° 39′ 21″	380	0.70908
GIR 16	*O. edulis*	Fornole	12° 27′ 16″	42° 32′ 48″	360	0.70909
GIR 17	*O. edulis*	Fornole	12° 27′ 16″	42° 32′ 48″	360	0.70908
GIR 18	*C. varia*	Fonte Nuova	12° 39′ 17″	41° 58′ 54″	60	0.70908
GIR 19	*B. harpula*	Fonte Nuova	12° 39′ 17″	41° 58′ 54″	60	0.70909
GIR 20	*Pecten jacobaeus*	S. Angelo Romano	12° 42′ 00″	42° 01′ 21″	130	0.70910
GIR 21	*P. jacobaeus*	S. Angelo Romano	12° 42′ 00″	42° 01′ 21″	130	0.70910
GIR 22	*A. ephippium*	Castel Chiodato	12° 41′ 58″	42° 03′ 32″	160	0.70910
GIR 23	*P. jacobaeus*	Terme di Cretone	12° 41′ 38″	42° 05′ 08″	70	0.70908
GIR 24	*Amusium cristatum*	Colle Calderino	12° 42′ 38″	42° 05′ 13″	140	0.70910
GIR 25	*A. cristatum*	Colle Calderino	12° 42′ 38″	42° 05′ 13″	140	0.70907
GIR 26	*A. cristatum*	Colle Calderino	12° 42′ 38″	42° 05′ 13″	140	0.70908
GIR 27	*A. ephippium*	Colle Sabato	12° 44′ 54″	42° 08′ 32″	170	0.70908
GIR 28	*O. edulis*	Colle Sabato	12° 44′ 54″	42° 08′ 32″	170	0.70908
GIR 29	*O. edulis*	Colle Sabato	12° 44′ 54″	42° 08′ 32″	170	0.70907
GIR 30	*S. brocchii*	Baschi Scalo	12° 08′ 22″	42° 41′ 30″	220	0.70907

Errors are expressed as two standard errors of the mean ($\pm 2 \times 10^{-5}$) for each value.

balthica FO). It is thus evident from this study the good correlation between the two independent dating methods, Sr isotope stratigraphy and biostratigraphy, for the Chiani–Tevere Formation. The resulting age of the UPS should be in the range of 1.65–1.50 Ma, corresponding to late Santernian (earliest early Pleistocene). The above results indicate that the UPS markers are almost isochronous.

Since the UPS represent features of late transgression and relative highstand within the MVT basin, it is likely that they are related to the eustatic sea level positions during the late Santernian. In the 1.65- to 1.50-Ma time interval, global sea level fluctuated with high-frequency (4th- and 5th-order cyclicity) between a lowstand at −78 m a.s.l. and a maximum at −19 m a.s.l., according to the global curve of Miller et al. (2005). This maximum, occurring at about 1.50 Ma (Miller et al., 2005), corresponds to the relative highstand in the MVT basin and slightly predates the early Pleistocene global eustatic peak. This peak occurred during the Emilian age at 1.40 Ma, according to Miller et al. (2005), or at 1.30 Ma according to Haq et al. (1987) (see also Pedley and Grasso, 2002). The imperfect correspondence between the local relative highstand (1.50 Ma) and the global eustatic peak (1.40–1.30 Ma) may be due to early uplift of sea bottom in the MVT basin during the Emilian (Mancini and Cavinato, 2005).

The projection of the altimetric position of the UPS along a NNW–SSE direction is shown in Figure 6. This plot reveals that the present elevation of the shorelines decreases from a maximum height of 480 m a.s.l. to the north to a minimum value of 220 m to the south, and that the lowering trend toward SSE appears almost linear.

The inferred age of the paleoshorelines is used to calculate the amount of regional uplift, which occurred after the formation of the UPS until now. The vertical velocities are calculated assuming: (1) an age resulting from isotopic and biostratigraphic data of 1.65–1.50 Ma; (2) an absolute initial sea level position, *sensu* Burbank and Anderson (2001), ranging from −78 and −19 m a.s.l., derived from Miller et al. (2005) eustatic sea level curve.

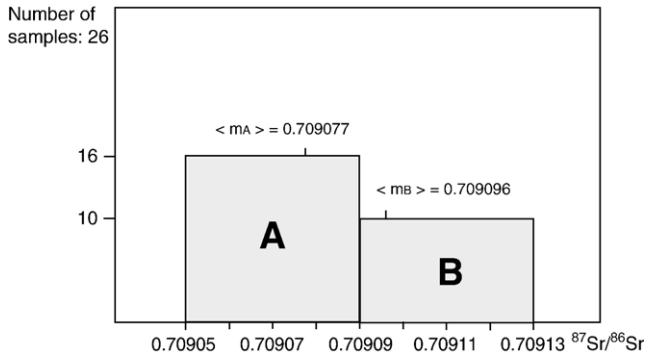

Figure 5. Histogram showing the distribution of measured $^{87}Sr/^{86}Sr$ ratios for the UPS samples, with values between 0.70907 and 0.70910. Both classes A and B encompass the error bar ($\pm 2 \times 10^{-5}$) of all the measured ratios; m_A and m_B are the mean values of each class.

https://doi.org/10.1016/j.yqres.2007.01.005 Published online by Cambridge University Press

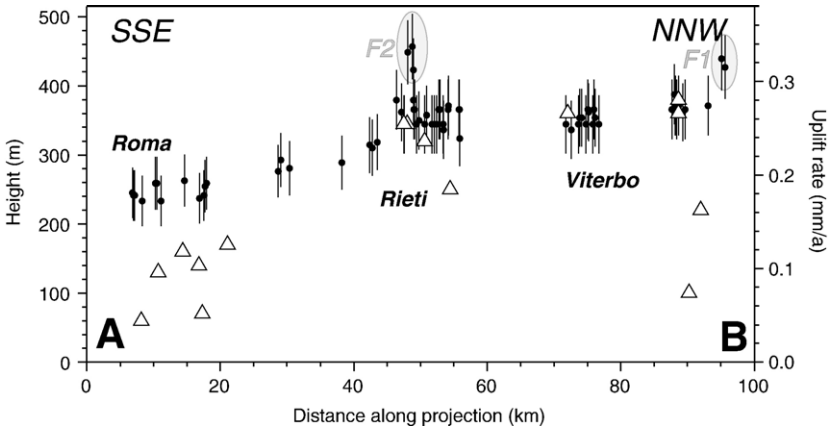

Figure 6. Projection of the altimetric position and uplift rate of the UPS (black dots with error bars) and sampled sites for Sr datings (white triangles) (trace of projection in Fig. 4). F1 and F2 are two groups of UPS outcrops vertically displaced by the activity of the Corbara and Sabina faults, respectively (see Fig. 1).

The amount of vertical uplift can be determined using the formula:

$$v = \frac{\Delta H}{\Delta T} = \frac{(H_1 - (H_0 \pm \delta H))}{T \pm \delta T},$$

where H_1 and H_0 are the actual and initial paleoshoreline altimetric position, in meters, with respect to the present sea level, and T is the paleoshorelines age. The resulting uplift rates, from the southernmost to the northernmost sector, range between 0.17±0.03 and 0.34±0.03 mm/a, respectively (Fig. 6).

The 100-km-long linear trend of the UPS and related uplift rates suggests that this differential uplift is probably due to regional movements, with the exception of two local anomalies, F1 and F2 (Fig. 6). These anomalies are present in the northernmost and central part of the UPS alignment at kilometer 95–100 and 50 on Fig. 6. They pertain to small sectors (< 10 km long) with respect to the 100-km-long trend. The first anomaly, F1 (km 95–100 of Fig. 6), can be examined at two outcrops at elevation 80 m higher than the adjacent sectors. This difference can be related to the activity of the NW–SE-trending Corbara Fault (Piccardi, 1993) (Fig. 1) that displaces the UPS, locally N–S oriented. The second anomaly, F2 (km 50 of Fig. 6), is due to the UPS outcropping at higher elevation with respect to neighboring sectors, with differences up to 100 m on a 10-km-long section of the plot. This offset is probably related to the activity of the well-known Sabina Fault (Fig. 1) (Alfonsi et al., 1991). Following Alfonsi et al. (1991), normal faulting related to this fault occurred prevalently during late early Pleistocene–middle Pleistocene (ending about 0.5 Ma). When considering the UPS age obtained in this work we may estimate a Sabina Fault slip rate of ~0.1 mm/a for the 1.5- to 0.5-Ma time interval.

More generally, the NNW–SSE-directed and SSW-dipping normal faults that border the MVT basin to the east (Fig. 1) might at some extent have provided both additional uplift to the footwall blocks, the "Peglia-Lucretili Ridge", and accommodation space to the axial part of the graben, the hanging wall block. This is commonly observed in extensional basins, as is the case in the Suez Graben (Jackson et al., 1988). However, the faults bordering the MVT did not contribute substantially to the UPS observed uplift and to basin subsidence during the early Pleistocene. In fact, (a) vertical displacements from faults of the eastern part of the basin do not exceed 150 m as a whole (Mancini and Cavinato, 2005), (b) lower Pleistocene sediments are up to 250–300 m in thickness and (c) the eastern margin of the MVT basin is lacking of typical fault-related depositional systems, such as Gilbert-type or slope-type fan deltas, which are common features of active grabens and half-grabens. Only shallow water fluvio-deltaic systems are present.

Comparison of the paleoshoreline data with other regional geological markers: inferences on character and shape of the uplift

As previously discussed, the UPS experienced a remarkable differential uplift highlighted by a clear elevation lowering towards the south. This characteristic may simply be due to a NW–SE regional trend of Central Apennines uplift, for example an along-chain trend. We test this hypothesis comparing the observed signal of the early Pleistocene UPS to other geological data present in the Latium region (Fig. 7). However, the only available dated geological marker with regional distribution is the upper Pleistocene marine terrace corresponding to Marine Isotope Stage 5e (125 ka), which discontinuously outcrops along the Tyrrhenian coast (Bordoni and Valensise, 1998; Nisi et al., 2003; Ferranti et al., 2006). A plot of the uplift rate along the Tyrrhenian coast, shown by this upper Pleistocene terrace, reveals that the Tyrrhenian coast remained stable at least for the last 125 ka, with exception of the Latium Volcanic Districts (Ceriti and Sabatini Mts and Albani Hills) where "peaks" are identified (see Fig. 9 in Bordoni and Valensise, 1998). This can be seen as a negative evidence for a NW–SE trend for the regional uplift profile, as inferred from the early Pleistocene UPS, whereas volcanism has exerted a major role in the local uplift of the upper Pleistocene terrace.

A possible influence of volcanism on uplift of the early Pleistocene UPS as a whole should be considered as well. In order to verify this effect, an altimetric plot of the Tiber River terraces, of the Giove Formation and of the principal volcanic formations in the MVT, compared with the UPS altitudinal

https://doi.org/10.1016/j.yqres.2007.01.005 Published online by Cambridge University Press

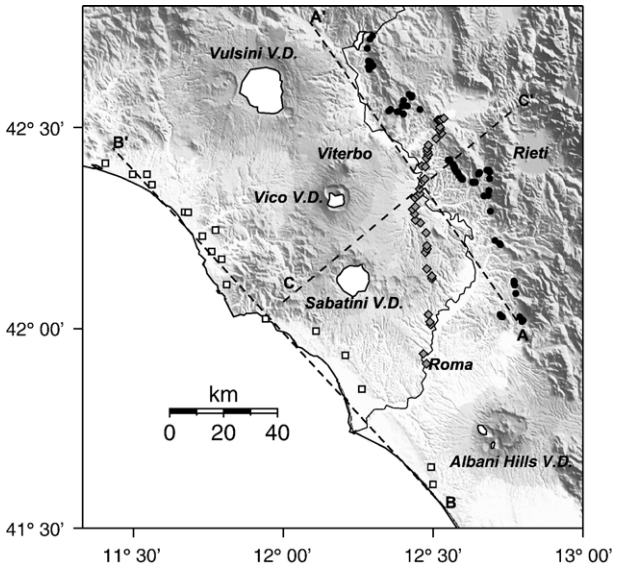

Figure 7. Map showing the location of the geological and geophysical data compared for uplift rate estimations: UPS (black dots); 5e marine terraces (white squares); geodetic leveling data (grey diamonds). A–A′ and B–B′ traces are shown on Figures 8a and b, respectively; for C–C′ see Figure 10.

trend, was constructed (Fig. 8A). The main emission centers, which locally uplifted in the middle-late Pleistocene, are also projected. The plot shows converging linear trends to the south, with no "bumps" clearly connected to magmatism. This figure also reveals that neither the fluvial terraces and distal volcanic units nor the UPS seem to have been significantly influenced by volcanic activity, whereas along the Tyrrhenian coast to the west the upper Pleistocene terrace is differentially uplifted, as result of volcanic activity (Bordoni and Valensise, 1998) (Fig. 8B).

Thus, considering that a differential uplift paralleling the Central Apennines seems to be unfavorable and no clear evidences exist about a major volcanic control on the UPS altitudinal trend, we decided to investigate an intriguing idea recently born for the southern sector of the Apenninic Chain. In fact, a symmetrically warped shape of uplift has been hypothesized for the Southern Apennines (Bordoni and Valensise, 1998). This chain sector is characterized by several geological markers that provide the best evidence for the Quaternary uplift in Italy. In this area, marine terraces and paleosurfaces of different age have been studied by various authors to estimate shape and amount of uplift (Cosentino and Gliozzi, 1988; Cinque et al., 1993; Bordoni and Valensise, 1998; Ascione and Romano, 1999; Amato and Cinque, 1999). It is suggested that the maximum uplift rate, with values up to 1 mm/a, is located in correspondence with the highest chain sectors along the divide. In contrast, minimum uplift rates are located in the peripheral sectors of the chain along the bordering pedemontane regions (Bordoni and Valensise, 1998). An important percentage of the actual topography of the chain is thus the result of the Quaternary uplift (Bordoni and Valensise, 1998; D'Agostino et al., 2001) and the resultant

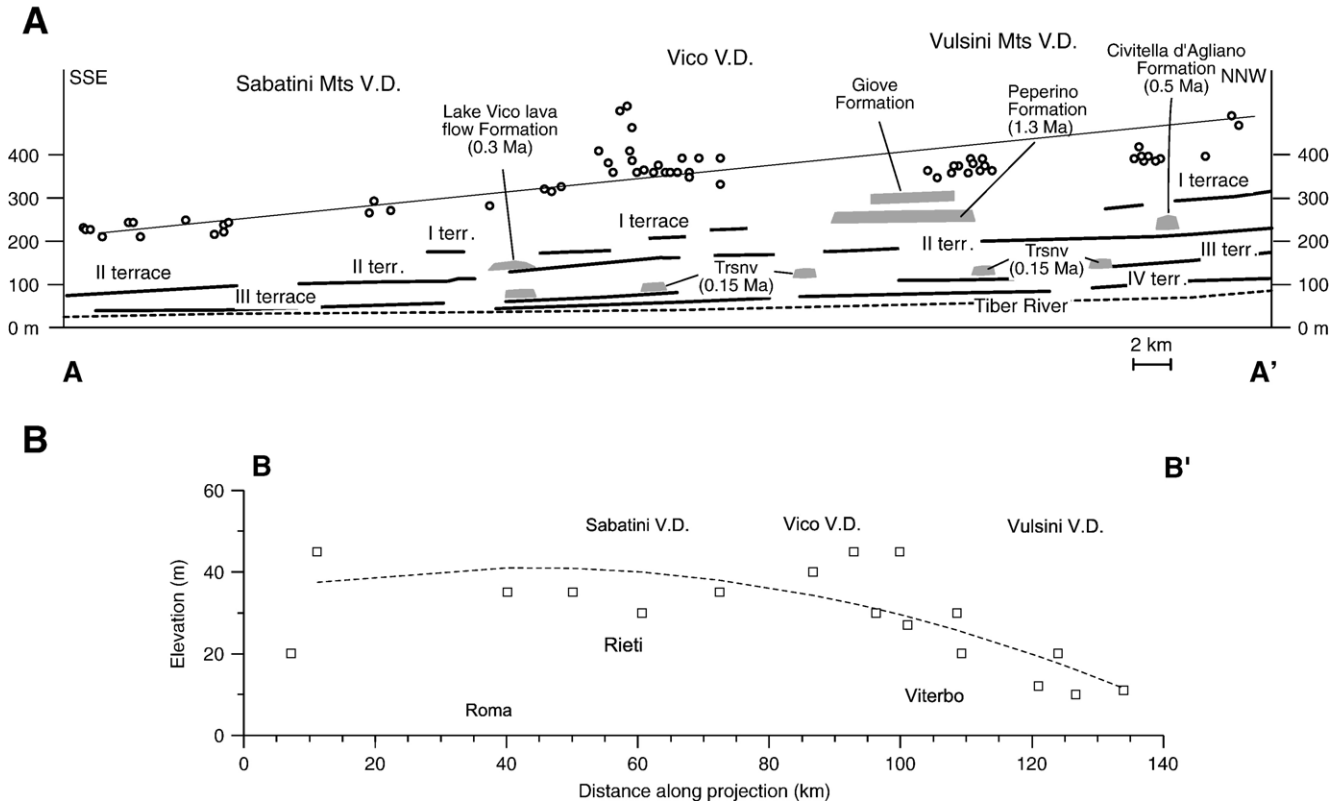

Figure 8. (A) projection of the altimetric position of the: UPS (white dots), Giove Formation, principal dated volcanic formations, Tiber River terraces (I to IV). Trsnv = *Tufo rosso a scorie nere vicano* Formation. (B) Projection of the altimetric position of the 5e marine terraces and related trendline (modified from Bordoni and Valensise, 1998). Traces of the projections A–A′ (A) and B–B′ (B) are shown in Figure 7.

https://doi.org/10.1016/j.yqres.2007.01.005 Published online by Cambridge University Press

pattern of uplift may be simplified with the symmetrical warped shape (Bordoni and Valensise, 1998).

Assuming a similar uplift trend for the Central Apennines, we consider the relation between the UPS altimetric position and the hypothesized warped uplift by means of the actual topography. A series of swath topographic profiles (A–A′ to E–E′ in Figs. 9A and B), perpendicular to the chain axis, allows us to reconstruct the "mean chain axis". The swath topographic profiles are therein constructed considering the elevation of points from 10-km-wide swaths, projected along the traces of N50°E oriented sections shown in Figure 9A and B. Maximum, minimum and mean elevations are calculated at regularly spaced intervals of 2 km (Fig. 9B). We have then considered as "mean chain axis" those zones of the swath profiles that lie on the highest topographic relief sectors of the chain. Considering the distance between the westernmost margin of the chain and the UPS alignment shown by profiles C–C′ to E–E′ (Fig. 9B), we notice that this distance increases as the altimetric position of the UPS decreases (Fig. 9C). This evidence can be considered as an indication that uplift values decrease away from the mean chain axis towards the sectors of low topographic relief. In our opinion, this negative correspondence enhances the possibility of a symmetrical warped shape of uplift also for the Central Apennines. It is interesting to notice that, on the Adriatic side of Central Apennines, an increasing uplift pattern moving from the coast to the chain (inland as much as 30–40 km) is inferred (Dufaure et al., 1988; Dramis, 1993; Centamore and Nisio, 2003), with values between 0.1 and 0.3–0.5 mm/a (Vannoli et al., 2004). The latter indication appears to be in a good agreement with our results, both in terms of signal magnitude and differential uplift trend.

Finally, we have compared our results against the current vertical movements given by original leveling data available in the study area (D'Anastasio, 2004; D'Anastasio et al., 2006) (Fig. 7). These comparative leveling data indicate relative vertical movements occurred between 1951 and 1997, referred to an arbitrary fixed point (in this case a benchmark located in the city of Rome). The velocities inferred from geodetic data and the geological uplift rate given by the UPS are plotted in Figure 10. Both data sets show similar signal trend and magnitude, with an increase of vertical velocities from SW to NE that is quite remarkable when it is taken into account that the time scale pertaining to each data set is very different (10^2 versus 10^6 years). Although leveling data used for the comparison are scattered and thus the obtained geodetic signal are not as well defined as the UPS uplift signal, it should be noticed that

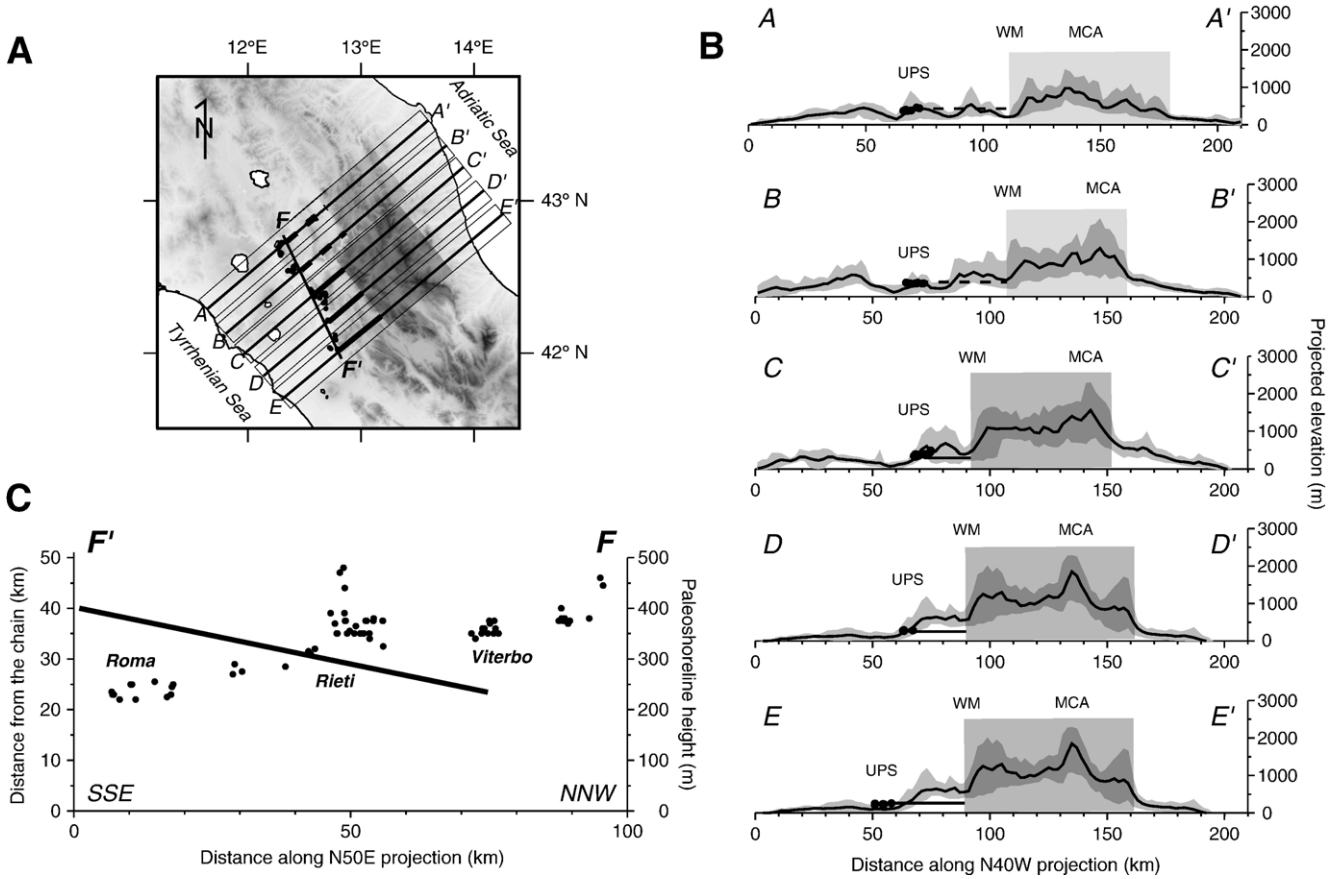

Figure 9. (A) Map of the swath topographic profile boxes (A–A′ to E–E′ traces) constructed in order to obtain the mean chain axis. Location of the UPS (black dots) and its trend alignment (F–F′) are also shown; (B) swath topographic profiles of sections A–A′ to E–E′. Shaded areas show the chain sectors of each profile: light and dark grey areas are referred to Northern and Central Apennines, respectively. WM = westernmost margin of the chain; MCA = mean chain axis; (C) UPS elevation vs. its distance from the westernmost margin of the chain, projected along the F–F′ trace of panel A. Note the reverse correlation between the UPS elevations and their distances from the chain for Central Apennines area.

https://doi.org/10.1016/j.yqres.2007.01.005 Published online by Cambridge University Press

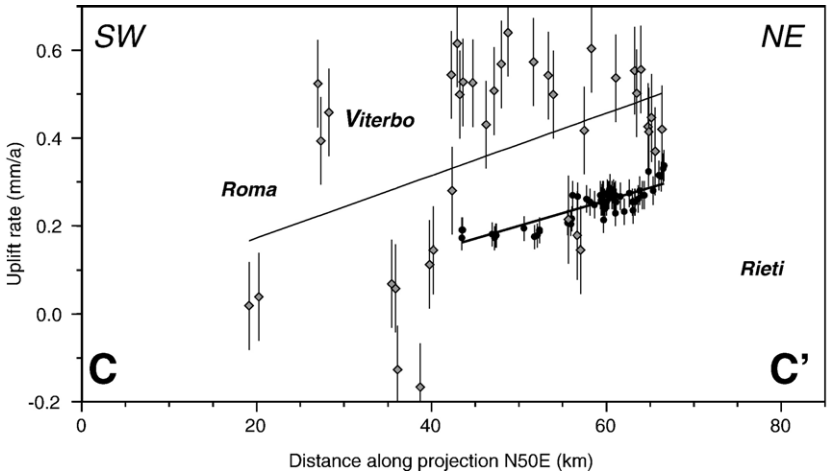

Figure 10. SW–NE projection of the uplift rate estimates deriving from UPS (black dots) and from geodetic leveling data (grey diamonds) (see Fig. 7 for their locations). Black and grey trendlines are from UPS and geodetic data, respectively. Trace of the projection is shown in Figure 7.

geodetic vertical velocities are higher with respect to those of the UPS (Fig. 10). In fact, geological velocities are here assumed as minimum rates, since we assume the UPS age as the starting time of regional uplift. However, indications of a substantial phase of a Central Apennines regional uplift younger than the UPS age could be found in Mancini et al. (2004) and Mancini and Cavinato (2005). Their geological and stratigraphical analysis of fluvial terraces of the Tiber River suggests that a clear increment of uplift may be set at about 1.2–1.0 Ma, after the deposition of the Giove Formation and of the volcanic Peperino Formation (1.30 Ma old) and before the aggradation of the first fluvial terrace, early-middle Pleistocene in age. If we assume that a significant increment of uplift of Central Apennines began in this time range, the geological estimates would be higher and closer to those given by geodetic data.

In conclusion, shape, length and continuity of the 100-km-long observed deformation point out the regional importance of the UPS as marker of uplift. The interpretation of the mechanism governing the regional tectonic signal is still a matter of debate in the scientific community, and several models, briefly reviewed in the following, have been proposed to explain the mechanism governing uplift and extension in the Apennines. Westaway (1993) and Hippolyte et al. (1994) suggest that uplift and extension in Southern Apennines are related to isostatic rebound of a detached lithosphere. A slab detachment was proposed by Spakman et al., 1993), but a slab detachment in this area is not sustained by tomographic studies, which show a continuous slab down to 350-km depth (Amato et al., 1993; Selvaggi and Chiarabba, 1995, among many others). Moreover, Giunchi et al. (1996), by the means of numerical modelling, suggest that slab detachment would cause subsidence and indicate that the uplift can be explained by slab retreat processes. On the other hand, Amato and Montone (1997) suggest that extension and uplift in Southern Apennines can be explained by a buoyant subducted continental lithosphere in the upper mantle. Another possible mechanism suggested in recent years asks for mantle upwelling, in response to slab retreat processes (Cavinato and De Celles, 1999; D'Agostino et al., 2001). For a comprehensive review of the proposed processes, see Amato and Montone (1997) and D'Agostino et al. (2001).

Our findings are expected to better constrain the Central Apennines Quaternary uplift and, together with already published and future works, to depict a more complete picture of this large-scale phenomenon. However, to discriminate the reliability of each causative mechanism proposed in the literature, an intensive modelling effort, which is out of the scope of this paper, will be necessary.

Concluding remarks

From Sr isotope analyses and from biostratigraphic data, the markers of the UPS in the Tiber Valley are in the range of 1.65–1.50 Ma. The UPS, which slowly decreases in the NNW–SSE direction from 480 to 220 m a.s.l., is isochronous all over its 100-km-long outcrop and slightly predates the inception of uplift of the Central Apennines. Corresponding uplift rates are in the range of about 0.34–0.17 ± 0.03 mm/a and linearly decrease in the NNW–SSE direction. A similar trend of uplift and uplift rate of this chain sector is recorded by geodetic leveling data.

The uplift of the Tiber Valley is considered to be regional as no relevant effects of volcanism are recorded from UPS. Moreover, a symmetrically warped shape of the regional uplift is suggested from the decreasing trend of uplift rates in the N–S direction, transverse to the mean axis of the Apennines.

Acknowledgments

We are grateful to Prof. Odoardo Girotti and Drs. Daniela Pantosti, Gian Paolo Cavinato, Roberto Basili and Nicola D'Agostino for helpful discussion. This paper has been strongly improved by the useful comments of reviewers, Profs. Mark Brandon and Ernesto Centamore, and editors Drs. Lewis Owen, Derek B. Booth and Susan Rasmussen. This work is partially funded by the "Dipartimento della Protezione Civile"-GNDT project "Probable earthquakes in Italy between year 2000 and 2030: guidelines for determining priorities in seismic risk

mitigation". Some of the figures were prepared by using GMT software package (Wessel and Smith, 1995).

References

Alfonsi, L., Funiciello, R., Mattei, M., Girotti, O., Maiorani, A., Martinez, M.P., Trudu, C., Turi, B., 1991. Structural and geochemical features of the Sabina strike-slip fault (Central Apennines). Bollettino della Società Geologica Italiana 110, 217–230.

Amato, A., Cinque, A., 1999. Erosional landsurfaces of the Campano-Lucano Apennines (S. Italy): genesis, evolution, and tectonic implications. Tectonophysics 315, 251–267.

Amato, A., Montone, P., 1997. Present-day stress field and active tectonics in southern peninsular Italy. Geophysical Journal International 130, 519–534.

Amato, A., Alessandrini, B., Cimini, G.B., Frepoli, A., Selvaggi, G., 1993. Active and remnant subducted slabs beneath Italy: evidence from seismic tomography and seismicity. Annali di Geofisica 36, 201–214.

Ambrosetti, P., Carboni, M.G., Conti, M.A., Esu, D., Girotti, O., La Monica, G.B., Landini, B., Parisi, G., 1987. Il Pliocene ed il Pleistocene inferiore del Bacino del Fiume Tevere nell'Umbria meridionale. Geografia Fisica e Dinamica Quaternaria 10, 10–33.

Antonioli, F., Ferranti, L., Kershaw, S., 2006. A glacial isostatic adjustment origin for double MIS 5.5 and Holocene marine notches in the coastline of Italy. Quaternary International 145–146, 19–29.

Ascione, A., Romano, P., 1999. Vertical movements on the eastern margin of Tyrrhenian extensional basin. New data from Mt. Bulgheria (Southern Apennines, Italy). Tectonophysics 315, 337–356.

Barberi, F., Buonasorte, G., Cioni, R., Fiordalisi, A., Foresi, L., Iaccarino, S., Laurenzi, M.A., Sbrana, A., Vernia, L., Villa, I.M., 1994. Plio-Pleistocene geological evolution of the geothermal area of Tuscany and Latium. Memorie Descrittive della Carta Geologica d'Italia 49, 77–134.

Bardaj, T., Dabrio, C.J., Goy, J.L., Somoza, L., Zazo, C., 1990. Pleistocene fan deltas in southeastern Iberian peninsula: sedimentary controls and-sea level changes. In: Colella, A., Prior, D.B. (Eds.), Coarse-Grained Deltas. IAS Spec. Publ., vol. 10, pp. 129–151.

Bartolini, C., 2003. Uplift and erosion: driving processes and resulting landforms. Editor Quaternary International 101–102, 280.

Bordoni, P., Valensise, G., 1998. Deformation of the 125 ka marine terrace in Italy: tectonic implications. In: Stewart, I.S., Vita-Finzi, C. (Eds.), "Coastal Tectonics". Special Publication-Geological Society of London, vol. 146, pp. 71–110.

Bromley, R.G., Asgaard, U., 1993. Two bioerosion ichnofacies produced by early and late burial associated with sea-level change. Geologische Rundschau 82, 276–280.

Burbank, D.W., Anderson, R.S., 2001. Tectonic Geomorphology. Blackwell Science, Oxford. 274 pp.

Cavinato, G.P., De Celles, P., 1999. Extensional basins in the tectonically bimodal central apennines fold-thrust belt, Italy: response to corner flow above a subducting slab in retrograde motion. Geology 27, 955–958.

Cavinato, G.P., Cosentino, D., De Rita, D., Funiciello, R., Parotto, M., 1994. Tectonic sedimentary evolution of intrappeninic basins and correlation with the volcano-tectonic activity in central Italy. Memorie Descrittive della Carta Geologica d'Italia 49, 63–75.

Centamore, E., Nisio, S., 2003. Effects of uplift and tilting in the Central–Northern Apennines (Italy). Quaternary International 101–102, 93–101.

Ciangherotti, A.D., Esu, D., Girotti, O., 1998. Review of the history of the Late Neogene-Early Quaternary non-marine molluscs of Italy. In: Van Kolfshoten, T., Gibbard, P.L. (Eds.), The Dawn of the Quaternary: Proceedings of the SEQS-EuroMam symposium 1996. Meded.-Ned. Inst. Toegepaste Geowet. TNO, vol. 60, pp. 491–498.

Cinque, A., Patacca, E., Scandone, P., Tozzi, M., 1993. Quaternary kinematic evolution of the Southern Apennines. Relationships between surface geological features and deep lithospheric structures. Annali di Geofisica 36, 249–260.

Cosentino, D., Gliozzi, E., 1988. Considerazioni sulle velocità di sollevamento dei depositi eutirreniani dell'Italia meridionale e della Sicilia. Memorie della Società Geologica Italiana 41, 653–665.

Cosentino, D., Miccadei, E., Parotto, M., 1993. Assetto geologico-strutturale dei Monti di Fara in Sabina (Lazio, Appennino centrale). Geologica Romana 29, 537–545.

D'Agostino, N., Jackson, J.A., Dramis, F., Funiciello, R., 2001. Interactions between mantle upwelling, drainage evolution and active normal faulting: an example from the central Apennines (Italy). Geophysical Journal International 147, 475–497.

D'Anastasio, E., 2004. Analisi e integrazione di dati geodetici ed elementi geologici per la definizione del campo di deformazione verticale a breve e lungo termine in Appennino (Italia). Ph.D. dissertation in Geophysics, XVI cycle, Dipartimento di Fisica, Università degli Studi di Bologna, 189 pp., Bologna.

D'Anastasio, E., De Martini, P.M., Selvaggi, G., Pantosti, D., Marchioni, A., Maseroli, R., 2006. Short-term vertical velocity field in the Apennines (Italy) revealed by geodetic levelling data. Tectonophysics 418, 219–234.

De Gibert, J.M., Martinell, J., Domènech, R., 1998. *Entobia* Ichnofacies in fossil rocky shores, Lower Pliocene, Northwestern Mediterranean. Palaios 13, 476–487.

Di Bella, L., Carboni, M.G., Bergamin, L., 2001. Pliocene–Pleistocene foraminiferal assemblages of the middle and lower Tiber Valley: stratigraphy and paleoecology. Geologica Romana (2000–2002) 36, 129–145.

Dramis, F., 1993. Il ruolo dei sollevamenti tettonici a largo raggio nella genesi del rilievo appenninico. Studi Geologici Camerti (1992/1), 9–15 (spec. Vol.).

Dufaure, J.J., Bossuyt, D., Rasse, M., 1988. Deformations Quaternaires et morphogenese de l'Apennin Central Adriatique. Phisio-Geo 18, 9–46.

Ferranti, L., Antonioli, F., Mauz, B., Amorosi, A., Dai Pra, G., Mastronuzzi, G., Monaco, C., Orrù, P., Pappalardo, M., Radtke, U., Renda, P., Romano, P., Sansò, P., Verrubbi, V., 2006. Markers of the last interglacial sea-level high stand along the coast of Italy: tectonic implications. Quaternary International 145–146, 30–54.

Funiciello, R., Parotto, M., 1978. Il substrato sedimentario nell'area dei Colli Albani: considerazioni geodinamiche e paleogeografiche sul margine tirrenico dell'Appennino centrale. Geologica Romana 17, 233–287.

Galadini, F., Galli, P., 2000. Active tectonics in the Central Apennines (Italy)—Input data for seismic hazard assessment. Natural Hazards 22, 225–270.

Galadini, F., Messina, P., Giaccio, B., Sposato, A., 2003. Early uplift history of the Abruzzi Apennines (central Italy): available geomorphological constraints. Quaternary International 101–102, 125–135.

Girotti, O., Mancini, M., 2003. Plio-Pleistocene stratigraphy and relations between marine and non-marine successions in the Middle Valley of the Tiber River (Latium, Umbria). Il Quaternario 16 (1 Bis), 89–106.

Girotti, O., Piccardi, E., 1994. Linee di riva del Pleistocene inferiore sul versante sinistro della media Valle del Fiume Tevere. Il Quaternario 7, 525–536.

Giunchi, C., Sabadini, R., Boschi, E., Gasperini, P., 1996. Dynamic models of subduction: geophysical and geological evidence in the Tyrrhenian. Geophysical Journal International 126, 555–578.

Haq, B.U., Hardenbol, J., Vail, P.R., 1987. Chronology of the fluctuating sea levels since the Triassic. Science 235, 1156–1167.

Hippolyte, J.C., Angelier, J., Roure, F., 1994. A major geodynamic change revealed by Quaternary stress patterns in the Southern Apennines (Italy). Tectonophysics 230, 199–210.

Hodell, D.A., Mead, G.A., Mueller, P.A., 1990. Variation in the strontium isotopic composition of seawater (8 Ma to present): implication for chemical weathering rates and dissolved fluxes to the oceans. Chemical Geology 80, 291–307.

Jackson, J.A., White, N.J., Garfunkel, Z., Anderson, H., 1988. Relations between normal-fault geometry, tilting and vertical motions in extensional terrains: an example from the southern Gulf of Suez. Journal of Structural Geology 10, 155–170.

Lajoie, K.R., 1986. Coastal tectonics. In: Wallace, R. (Ed.), Active Tectonics. National Academy Press, Washington, pp. 95–124.

Little, C., 2000. The Biology of Soft Shores and Estuaries. Oxford Univ. Press, Oxford. 252 pp.

Locardi, E., Funiciello, R., Lombardi, G., Parotto, M., 1977. The main volcanic groups of Latium (Italy): relations between structural evolution and petrogenesis. Geologica Romana 15, 279–300.

Malatesta, A., 1974. Malacofauna pliocenica umbra. Memorie Descrittive della Carta Geologica d'Italia 13, 1–464.

Malatesta, A., Zarlenga, F., 1986. Evoluzione paleogeografico-strutturale plio-pleistocenica del basso Bacino romano e a Sud del Tevere. Memorie della Società Geologica Italiana 35, 75–98.

Malinverno, A., Ryan, W.B.F., 1986. Extension in the Tyrrhenian Sea and shortening in the Apennines as a result of arc migration driven by sinking of the lithosphere. Tectonics 5, 227–245.

Mancini, M., 2000. Stratigrafia dei depositi fluviali e costieri pleistocenici nella Media Valle del Tevere. PhD dissertation in Earth Science, XII cycle, Dip. Scienze della Terra, Università degli Studi di Roma "La Sapienza", 211 pp., Rome.

Mancini, M., Cavinato, G.P., 2005. The Middle Valley of the Tiber River, central Italy: Plio-Pleistocene fluvial and coastal sedimentation, extensional tectonics and volcanism. In: Blum, M.D., Marriott, S., Leclair, S. (Eds.), Fluvial Sedimentology VII. IAS Spec. Publ., vol. 35, pp. 373–396.

Mancini, M., Girotti, O., Cavinato, G.P., 2004. Il Pliocene e il Quaternario della Media Valle del Tevere. Geologica Romana (2003–2004) 37, 175–236.

Massari, F., Parea, G.C., 1988. Progradational gravel beach sequences in a moderate- to high-energy, microtidal environment. Sedimentology 35, 881–913.

Miller, K.G., Kominz, M.A., Browning, J.V., Wright, J.D., Mountain, G.S., Katz, M.E., Sugarman, P.J., Cramer, B.S., Christie-Blick, N., Pekar, S.F., 2005. The phanerozoic record of global sea-level change. Science 310, 1293–1298.

Montone, P., Amato, A., Pondrelli, S., 1999. Active stress map of Italy. Journal of Geophysical Research 104, 25595–25610.

Nisi, M.F., Antonioli, F., Dai Pra, G., Leoni, G., Silenzi, S., 2003. Coastal deformation between the Versilia and the Garigliano plains (Italy) since the last interglacial stage. Journal of Quaternary Science 18 (8), 709–721.

Nybakken, J.W., 2001. Marine Biology: An Ecological Approach, 5th edition. Benjamin Cummings, San Francisco. 516 pp.

Parotto, M., Praturlon, A., 1975. Geological summary of the Central Apennines. CNR-Quaderni de La Ricerca Scientifica 90, 257–311.

Pasini, G., Colalongo, M.L., 1994. Proposal for the erection of the Santernian/Emilian boundary stratotype (Lower Pleistocene) and new data on the Pliocene/Pleistocene boundary-stratotype. Bollettino della Società Paleontologica Italiana 33, 101–120.

Patacca, E., Scandone, P., 2001. Late thrust propagation and sedimentary response in the thrust-belt-foredeep system of the Southern Apennines (Pliocene–Pleistocene). In: Vai, G.B., Martini, I.P. (Eds.), Anatomy of an Orogen: the Apennines and Adjacent Mediterranean Basins. Kluwer Academic Publishers, Great Britain, pp. 401–440.

Patacca, E., Sartori, R., Scandone, P., 1992. Tyrrhenian Basin and Apenninic Arcs: kinematics relations since Late Tortonian time. Memorie della Società Geologica Italiana 45, 425–451.

Pedley, M., Grasso, M., 2002. Lithofacies modelling and sequence stratigraphy in microtidal cool-water carbonates: a case study from the Pleistocene of Sicily, Italy. Sedimentology 49, 533–553.

Piccardi, E., 1993. Il Plio-Pleistocene in sinistra del Tevere dal Lago di Corbara a Magliano in Sabina. PhD dissertation in Earth Science, V cycle, Dip. Scienze della Terra, Università degli Studi di Roma "La Sapienza", 210 pp., Rome.

Pondrelli, S., Morelli, A., Ekström, G., Mazza, S., Boschi, E., Dziewonski, A.M., 2002. European–Mediterranean regional centroid moment tensors: 1997–2000. Physics of the Earth and Planetary Interiors 130, 71–101.

Reading, H.G., Collinson, J.D., 1996. Clastic coasts, In: Reading, H.G. (Ed.), Sedimentary Environments: Processes, Facies and Stratigraphy, 3rd edition. Blackwell Science, Oxford, pp. 154–231.

Selvaggi, G., Chiarabba, C., 1995. Seismicity and P-wave velocity image of the Southern Tyrrhenian subduction zone. Geophysical Journal International 121, 818–826.

Spakman, W., van der Lee, S., van der Hilst, R., 1993. Travel-time tomography of the European–Mediterranean mantle down to 1400 km. Physics of the Earth and Planetary Interiors 79, 3–74.

Summerfield, M.A., 1991. Global Geomorphology. Longman, Singapore. 537 pp.

Valensise, G., Pantosti, D., 2001a. The investigation of potential earthquake sources in peninsular Italy: a review. Journal of Seismology 5, 287–306.

Valensise, G., Pantosti, D., 2001b. Database of Potential Sources for earthquakes larger than M 5.5 in Italy. Annali di Geofisica 44 (4), 964 (suppl.).

Vannoli, P., Basili, R., Valensise, G., 2004. New geomorphic evidence for anticlinal growth driven by blind-thrust faulting along the northern Marche coastal belt (central Italy). Journal of Seismology 8 (3), 297–312.

Wessel, P., Smith, W.H.F., 1995. New version of the Generic Mapping Tools released. Eos Transactions AGU 76 (33), 329.

Westaway, R., 1993. Quaternary uplift of Southern Italy. Journal of Geophysical Research 97, 15437–15464.